VIP Asymmetric Biomineralization

DOI: 10.1002/anie.201105445

Formation of Enantiomeric Impeller-Like Helical Architectures by DNA Self-Assembly and Silica Mineralization**

*Ben Liu, Lu Han, and Shunai Che**

The study and mimicking of the self-assembly of biomolecular building blocks in biological organisms to construct well-defined two- and three-dimensional (2D and 3D) mesostructures and macroscopic architectures has recently attracted significant attention in natural and materials sciences. The objective of these studies are not only to better understand the mechanism leading to the formation of structures found in living organisms, but also to assist applications in biotechnology, nanotechnology, and materials chemistry.[1] Chirality and induced superhelicity are among the most intriguing phenomena in biological organisms.[2] As a central biomolecule in living organisms, DNA is one of the most attractive "building blocks", because of its double-stranded helical structure with well-defined minor and major grooves, well-regulated micrometer length and uniform diameter of about 2 nm. Positively charged counterion/supramolecule-induced DNA packing structures can be found in almost all living forms. Various DNA liquid crystal phases, including isotropic, blue, cholesteric, columnar, hexagonal, and crystalline phases, have been discussed extensively.[3] It is worth noting that the coexistence and competition between the long-range chiral cholesteric arrangement and the 2D-columnar packing of DNA has been found both in vivo and in vitro.[4] The chiral cholesteric structure and phase competition behaviors are known to be sensitive to counter ion strength, concentration, temperature, pressure, pH value, and other parameters.[3f,g,5] However, the replication of chiral DNA packing with inorganic materials has not been previously reported.

Silicon and oxygen are the most abundant elements in the Earth's crust.[6] Diatoms, radiolarians, and sponges are the main sources of amorphous organic silica complexes, and produce intricate 3D nano- and microstructures with a precision and detail far exceeding current human engineering capabilities.[7] However, reports on DNA directed silica mineralization replication are extremely rare, because of the well-known difficulty that negatively charged silica species do not interact with DNA polyanions at pH values of 4.3–11.9,[8] the range at which the double-helical configuration of DNA can be maintained.[9]

Herein, we describe our efforts to synthesize chiral DNA–silica complex (DSC) in the presence of alkaline earth metal ions. The DSCs were fully characterized by structural and morphological analysis using electron microscopy, which was made possible by the framing of the DNA packing structures in a rigid silica wall. The reversible behavior of DNA chiral packing and the corresponding macroscopic helical morphologies were investigated by X-ray diffraction (XRD), solid-state diffuse-reflectance circular dichroism (DRCD), scanning electron microscopy (SEM) and high-resolution transmission electron microscopy (HRTEM).

The formation of DSCs was based on the co-structure directing effect of *N*-trimethoxysilylpropyl-*N*,*N*,*N*-trimethylammonium chloride (TMAPS).[10] The positively charged quaternary ammonium group of TMAPS acts not only as a co-structure directing agent, but also as a condensing agent for DNA, and the silane site is able to co-condense with a silica source, such as tetraethoxysilane (TEOS), to achieve the subsequent assembly of a silica framework. The trimethylene groups of TMAPS covalently tether the silicon atoms incorporated into the framework to the cationic ammonium groups, regardless of the type of charge on the silicate. In our previous work, we have found that an exceptionally small interaxial separation of about 25 Å was formed upon quaternary ammonium phosphate electrostatic "zipping" along the DNA–DNA contacts,[11] and the silica wall formed between DNA molecules in the diagonal position were optimal for the formation of a 2D-square *p4mm* structure.[12]

Alkaline earth metal ions are known to interact with the phosphate group of DNA, by electrostatic or hydrogen bonding of the coordinating water molecules that surround the metal ions.[13] DNA chiral aggregation (including the formation of liquid crystal phases) can be induced by adding these metal ions to solutions of DNA.[3f,g] This effect has been attributed to the linkage of two different DNA sites, and the dislocated array of DNA molecules possesses an intrinsic tendency to self-organize into cholesteric mesophases or microdomains.

Herein, we successfully synthesized enantiomeric impeller-like helical DNA-silica complexes (IHDSCs) by introducing various alkaline earth metal ions into the co-structure-directed synthesis. Sonicated DNA ranging between 100 and 300 bp in length was used, as confirmed by 1% agarose gel electrophoresis (Supporting Information, Figure S1). Mono- and divalent metal ions (alkali metals and alkaline earth

[*] B. Liu,[+] Dr. L. Han,[+] Prof. S. Che
School of Chemistry and Chemical Engineering
State Key Laboratory of Metal Matrix Composites
Shanghai Jiao Tong University
800 Dongchuan Road, Shanghai, 200240 (P.R. China)
E-mail: chesa@sjtu.edu.cn
Homepage: http://che.scct.sjtu.edu.cn/Che/HOME.html

[+] These authors contributed equally to this work.

[**] We acknowledge the support of the National Natural Science Foundation of China (Grant No. 20821140537), the 973 project (2009CB930403), and Grand New Drug Development Program (No. 2009ZX09310-007) of China.

Supporting information for this article, including the synthesis and characterization of the DNA–silica complex and DNA liquid crystal, is available on the WWW under http://dx.doi.org/10.1002/anie.201105445.

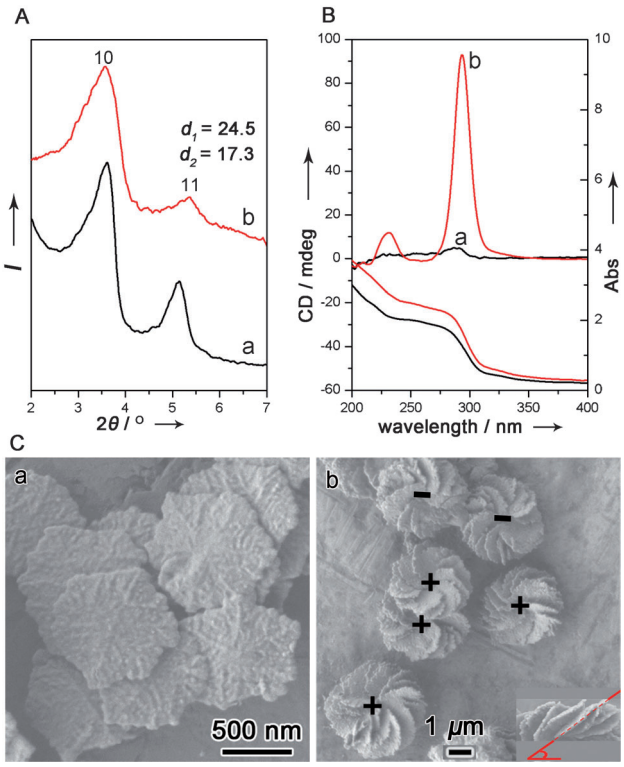

Figure 1. Structures and morphologies of the DSCs. A) XRD patterns, B) DRCD and UV/Vis spectra, and C) SEM images of the DSCs synthesized a) without and b) with addition of Mg^{2+} ions at 0 °C. Inset of SEM image (C b): SEM image taken from the direction perpendicular to the impeller axis. Left- and right-handed impellers are denoted by + and −, respectively. The synthesis molar composition of DNA/$MgCl_2$/TMAPS/TEOS/H_2O is 1:*x*:3.5:15:18 000, where *x* = 0 (a) and 1 (b). The pH value of both synthesis solutions was 5.20.

metals) and some transition-metal ions (in the form of salts), as well as amino acids, were introduced into the DSC synthesis (Supporting Information, Figure S2, S3). Figure 1 A shows the XRD patterns of the samples synthesized without and with Mg^{2+} ions at 0 °C. Both samples revealed two well-resolved reflections in the range $2\theta = 3$–6°, with a *d*-spacing ratio of $\sqrt{2}$. These were indexed as 10 and 11 reflections of a 2D-square lattice with a unit cell parameter of $a \approx 2.5$ nm, indicating that both samples had highly ordered mesostructures. Figure 1 B shows the DRCD and UV/Vis spectra of the samples shown in Figure 1 A. No DRCD signal was observed for the sample synthesized in the absence of metal ion, indicating the absence of a long-range DNA chiral arrangement. Interestingly, two strongly positive DRCD signals were observed at around 230 and 295 nm for the sample synthesized in the presence of Mg^{2+} ion . This indicates the existence of right-handedness in the DNA superhelical interaction, similar to the nonconservative ellipticities exhibited for chiral cholesteric organization.[3f,g,14,15]

Figure 1 C shows the macroscopic morphologies of these two samples. The DSCs synthesized in the absence of metal ions are composed of hexagonal platelets.[12] The sample synthesized in the presence of Mg^{2+} ions showed an extraordinary impeller-like helical morphology, which had a uniform diameter of about 4 μm and a uniform thickness of about 100 nm (the thickness of the blades). The blades grew from the center of the impeller and stacked in a single direction, which reveals unambiguously the handedness of the helical morphology (Supporting Information, Figure S4). The IHDSC with blades arranged in a clockwise manner is defined as left-handed and that with a counterclockwise arrangement is defined as right-handed. To express enantiopurity, the enantiomeric excess (*ee*) was defined by 100 % × [(l−r)/(l+r)], where l and r are the amount of the left- and right-handed IHDSC in a given sample. The *ee* was estimated by counting the characteristic morphologies of more than 500 randomly chosen particles in the SEM images, obtained in over 10 different regions of the sample holder. The IHDSCs synthesized at 0 °C were found to be predominantly left-handed, with an absolute *ee* of about 50 %. According to the corresponding positive CD signals, it can be concluded that the DNA has a right-handed long-range chiral packing in the left-handed impeller. The number of blades in each impeller ranged from 8 to 14. The blades were in different inclination angles in the range of 25–35° (insert in Figure 1 C b) and consequently the pitch length was calculated to be 20–30 μm.

In the presence of Mg^{2+} ions, IHDSCs with highly ordered 2D-square *p4mm* structures can be synthesized with different TMAPS/DNA molar ratios, as revealed by XRD patterns (Supporting Information, Figure S5). It is interesting to note that the handedness of the IHDSCs changed depending on the quaternary ammonium/phosphate ratio, and was reversed at higher ratios. As shown in Figure 2 A, the left-handed impeller-like helical DSC content, denoted by +, decreased with increasing TMAPS/DNA molar ratios. Enantiomeric impellers with *ee* values of 50, 25, 10, −5, and −15 % were observed with TMAPS/DNA molar ratios of 3.5, 4.5, 5.5, 6.5, and 7.5, respectively. This result unambiguously revealed the reversal of handedness from predominantly left-handed to right-handed impellers achieved by controlling the interaction between quaternary ammonium group of TMAPS and phosphate of DNA.

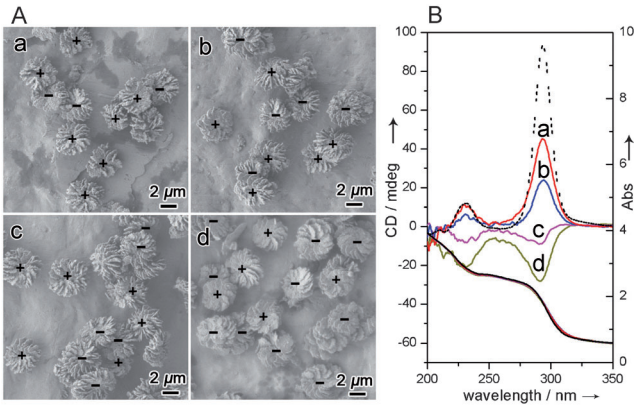

Figure 2. Reversal of the handedness of IHDSCs with increasing TMAPS/DNA molar ratio at 0 °C. A) SEM images and B) DRCD and UV/Vis spectra of the IHDSCs synthesized with TMAPS/DNA molar ratios of 3.5 (dotted line, also shown in Figure 1 B b), a) 4.5, b) 5.5, c) 6.5, and d) 7.5. The left- and right-handed impeller are denoted by + and −, respectively. The synthesis molar composition of DNA/$MgCl_2$/TMAPS/TEOS/H_2O is 1:1:*x*:15:18 000. The pH value of synthesis solutions was 5.20.

From DRCD, it can be seen that the intensity of the positive DRCD signals at around 230 and 295 nm decreased when the TMAPS/DNA molar ratio was increased from 3.5 to 5.5 (Figure 2B). This implies that the extent of right-handed DNA packing had decreased, although the right-handed excess was maintained. This result consists with the decrease in impeller morphological *ee* values observed, from 50 to 10% (that is, the extent of left-handed impeller decreased). When the TMAPS/DNA molar ratio was further increased from 5.5 to 7.5, the DRCD signals inverted to negative DRCD signals and then gradually increased in intensity. The IHDSCs with right-handed excess ($ee = -15\%$) show two strongly negative DRCD signals, which are exactly opposite to the DRCD signals observed for the left-handed helical excess IHDSCs (Figure 2B, dotted line). This result indicates that the DNA packing has the opposite long-range chirality in the two samples. These results were completely consistent with a change in the IHDSCs from a left-handed to a right-handed architecture, indicating that the handedness of the impellers reflects the DNA packing chirality. This observation also indicates that the handedness of DNA packing is affected by TMAPS/DNA molar ratio.

IHDSCs with highly ordered 2D-square *p4mm* structures can be synthesized over a wide temperature range, from 0 to 40°C, as revealed by XRD patterns (Supporting Information, Figure S6). As shown in Figure 3, the handedness of the IHDSCs changes depending on the reaction temperature, and was finally reversed at higher temperatures. Enantiomeric impellers with *ee* values of 50, 10, −10, −40, and −80% were observed at synthesis temperatures of 0, 4, 8, 15, and 25°C, respectively. The corresponding positive nonconservative DRCD signals showed a right-handed DNA chiral packing mesostructure, a result that was inverted when the temperature was increased. The sample synthesized at 25°C was composed almost exclusively of right-handed impellers, indicating that elevated temperatures were favorable to the formation of the right-handed IHDSCs. Changing the pH value of the synthetic mixture also gave rise to reversal of the handedness for DNA chiral packing structure and the corresponding macroscopic IHDSC morphology (Supporting Information, Figure S7).

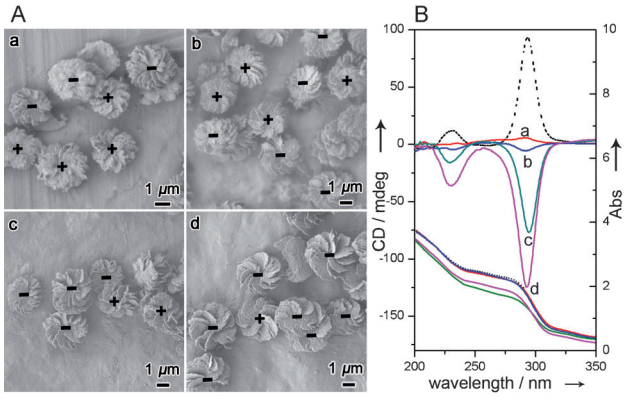

Figure 3. Reversal of the handedness of IHDSCs with increasing temperature. A) SEM images and B) DRCD and UV/Vis spectra of the IHDSCs synthesized at 0 (dotted line, also shown in Figure 1Bb), a) 4, b) 8, c) 15, and d) 25°C. The left- and right-handed impeller are denoted by + and −, respectively. The synthesis molar composition of DNA/$MgCl_2$/TMAPS/TEOS/H_2O is 1:1:3.5:15:18000. The pH value of synthesis solutions was 5.20.

From the above results, it can be deduced that chiral 2D-square structured DNA packing gave rise to the formation of IHDSCs. The *p4mm* domains formed by DNA–DNA "zippers" prefer to form a flat morphology and cannot accommodate a large twist angle, which would force the edge of the DSC into a bent conformation. With further silica condensation, several bending *p4mm* domains on the edges cannot coexist, damaging the integrity of the rigid DSC platelet and inducing the breakage of the edges into multiple blades. This leads to the formation of IHDSCs connected together in the center, and subsequent growth along the bent blades leads to the graceful impeller-like helical architecture. It is not difficult to imagine that in left-handed IHDSC the *p4mm* structured DNA columns are in the right-handed twisted stacking, with a certain twist angle for each layer, and vice versa for the right-handed IHDSC (Scheme 1).

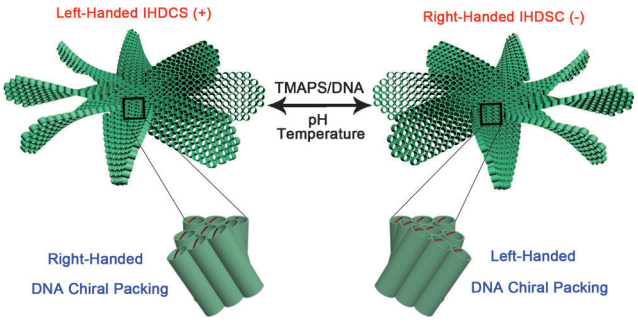

Scheme 1. Illustration of the macroscopic enantiomeric helical morphologies and corresponding opposite DNA chiral packing of the impeller-like helical DNA-silica complexes (IHDSCs).

To explore the intrinsic nature of the IHDSCs, detailed HRTEM observations were carried out. All IHDSCs showed highly ordered 2D-square *p4mm* structures at both their center, and in the blades, by TEM (Supporting Information, Figure S8). Meanwhile, it was observed that the blades were often bent and only aligned with the incident electron beam in a local region. A single blade taken from the sample synthesized at 25°C (Supporting Information, Figure S9), which was formed by crushing the sample before analysis, was carefully checked by HRTEM. Figure 4 shows the low-magnification TEM image and the HRTEM image of the enlarged top part, and clearly shows the highly ordered 2D-square lattice. As expected, the crystal structure was found to be slightly bent along the (01) plane. It showed a 1D fringe along the middle of the blade, and finally became completely misaligned contrast at the bottom (Supporting Information, Figure S10). By tilting the blade along its (10) axes by 10.28° and then 9.51°, the middle and bottom parts could be well aligned, showing a highly ordered 2D-square contrast. Therefore, the DNA columnar packing structure twisted in the (01) lattice plane continuously in a left-handed manner. This reveals the presence of a large-scale regular left-handed twist, which corresponds to the results of DRCD. The orientation of

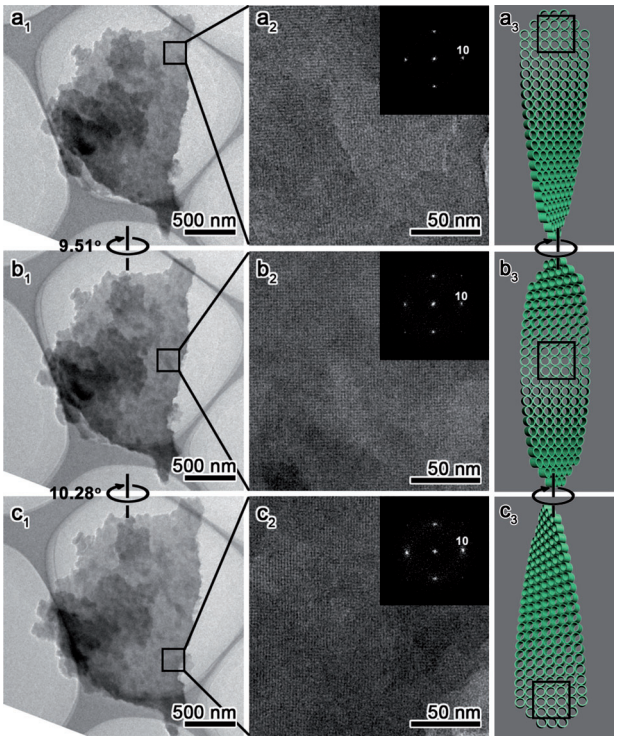

Figure 4. Left-handed DNA chiral packing structure in the right-handed IHDSC shown in Figure 3d. The blades are bended and the 2D-square lattice can only align to the incident electron beam in the top region (a1–a3). The middle (b1–b3) and bottom (c1–c3) parts have been aligned by tilting the crystal along its (10) axes by 10.28° and then 9.51°, respectively, and shows a left-handed DNA chiral packing.

the blades diverged slightly, revealing a splay of an extremely small tilting angle per layer of about 0.035°, while the pitch length was as large as 26 μm, which is consistent with results from SEM observations.

The handedness of the DNA packing was found to be inverted from right-handed to left-handed with increasing TMAPS/DNA molar ratio, suggesting that the strong interaction between the quaternary ammonium groups and the phosphate groups of DNA stabilizes left-handed DNA packing. The quaternary ammonium group of TMAPS not only links the silica species to the DNA molecules, but also acts as a condensing agent and changes the DNA packing behavior. The effect of increasing the temperature and pH of the synthesis can be attributed to increase in the interaction strength between the quaternary ammonium group of TMAPS and the phosphate of DNA (Supporting Information, Figure S11). Silica species are negatively charged (I^-) when operating at pH values higher than the isoelectric point of silica (pH ≈ 2), and the DSC is formed through a DNA-N^+–I^- interaction, where the quaternary ammonium group is covalently bound to the charged silica species (I^-). The positively charged quaternary ammonium group mediates between both negatively charged phosphate and silicate species. Increasing the temperature of the synthesis facilitates silicate condensation and causes the negative charge density of the silicate network to decrease. This leads to a decrease in the interaction between the quaternary ammonium groups and the negative silicate species, while simultaneously enhancing the interaction between the negative phosphate and the quaternary ammonium group. At higher pH values, the charge density of the phosphate is increased. This also enhances the interaction between DNA and the quaternary ammonium groups. The reversal of the long-range chiral organization from intrinsically right-handed into an induced left-handed conformation leads to a change in the morphology of IHDSCs from left- to right-handed.

To the best of our knowledge, this is the first example of DNA chiral liquid-crystal-phase silica mineralization and the first formation of IHDSCs with enantiomeric helical architectures. We expect that the insight gained into meso- and macroscopic DNA packing will facilitate both the exploration of DNA packing theory with addressable biological molecular interactions and the creation of new classes of ordered helical materials.

Received: August 2, 2011
Revised: October 18, 2011
Published online: December 23, 2011

Keywords: chirality · DNA condensation · helix reversal · self-assembly · silica mineralization

[1] H. Cölfen, S. Mann, *Angew. Chem.* **2003**, *115*, 2452–2468; *Angew. Chem. Int. Ed.* **2003**, *42*, 2350–2365.
[2] L. Pérez-García, D. B. Amabilino, *Chem. Soc. Rev.* **2002**, *31*, 342–356.
[3] a) V. A. Bloomfield, *Curr. Opin. Struct. Biol.* **1996**, *6*, 334–341; b) I. Koltover, T. Salditt, J. O. Rädler, C. R. Safinya, *Science* **1998**, *281*, 78–81; c) A. Leforestier, F. Livolant, *Biophys. J.* **1993**, *65*, 56–72; d) F. Livolant, A. Leforestier, *Prog. Polym. Sci.* **1996**, *21*, 1115–1164; e) F. Livolant, A. Levelut, J. Doucet, J. Benoit, *Nature* **1989**, *339*, 724–726; f) Z. Reich, S. Levin-Zaidman, S. B. Gutman, T. Arad, A. Minsky, *Biochemistry* **1994**, *33*, 14177–14184; g) Z. Reich, E. J. Wachtel, A. Minsky, *Science* **1994**, *264*, 1460–1463; h) J. P. Straley, *Phys. Rev. A* **1976**, *14*, 1835–1841.
[4] a) R. D. Kamien, D. R. Nelson, *Phys. Rev. Lett.* **1995**, *74*, 2499–2502; b) R. D. Kamien, D. R. Nelson, *Phys. Rev. E* **1996**, *53*, 650–666; c) A. Leforestier, A. Bertin, J. Dubochet, K. Richter, N. Sartori Blanc, F. Livolant, *C. R. Chim.* **2008**, *11*, 229–244; d) F. Livolant, A. Leforestier, *Biophys. J.* **2000**, *78*, 2716–2729.
[5] G. Yan, T. C. Lubensky, *J. Phys. II* **1997**, *6*, 1023–1034.
[6] J. J. R. F. Da Silva, R. J. P. Williams, *The biological chemistry of the elements: the inorganic chemistry of life*, Oxford University Press, Oxford, **2001**.
[7] R. L. Brutchey, D. E. Morse, *Chem. Rev.* **2008**, *108*, 4915–4934.
[8] a) C. Jin, H. Qiu, L. Han, M. Shu, S. Che, *Chem. Commun.* **2009**, 3407–3409; b) M. Numata, K. Sugiyasu, T. Hasegawa, S. Shinkai, *Angew. Chem.* **2004**, *116*, 3341–3345; *Angew. Chem. Int. Ed.* **2004**, *43*, 3279–3283.
[9] H. Millonig, J. Pous, C. Gouyette, J. A. Subirana, J. L. Campos, *J. Inorg. Biochem.* **2009**, *103*, 876–880.
[10] a) S. Che, A. E. Garcia-Bennett, T. Yokoi, K. Sakamoto, H. Kunieda, O. Terasaki, T. Tatsumi, *Nat. Mater.* **2003**, *2*, 801–805; b) S. Che, Z. Liu, T. Ohsuna, K. Sakamoto, O. Terasaki, T. Tatsumi, *Nature* **2004**, *429*, 281–284.
[11] a) S. Chesnoy, L. Huang, *Annu. Rev. Biophys. Biomol. Struct.* **2000**, *29*, 27–47; b) H. M. Evans, A. Ahmad, K. Ewert, T. Pfohl, A. Martin-Herranz, R. Bruinsma, C. Safinya, *Phys. Rev. Lett.* **2003**, *91*, 075501; c) H. M. Harreis, C. N. Likos, H. Löwen,

Biophys. J. **2003**, *84*, 3607 – 3623; d) A. Kornyshev, S. Leikin, *Phys. Rev. Lett.* **1999**, *82*, 4138 – 4141.
[12] C. Jin, L. Han, S. Che, *Angew. Chem.* **2009**, *121*, 9432 – 9436; *Angew. Chem. Int. Ed.* **2009**, *48*, 9268 – 9272.
[13] a) L. Berti, G. A. Burley, *Nat. Nanotechnol.* **2008**, *3*, 81 – 87; b) V. A. Bloomfield, *Biopolymers* **1991**, *31*, 1471 – 1481; c) J. G. Duguid, V. A. Bloomfield, *Biophys. J.* **1995**, *69*, 2642 – 2648; d) R. M. Izatt, J. J. Christensen, J. H. Rytting, *Chem. Rev.* **1971**, *71*, 439 – 481; e) N. Sundaresan, C. H. Suresh, T. Thomas, T. Thomas, C. Pillai, *Biomacromolecules* **2008**, *9*, 1860 – 1869.
[14] a) C. Bustamante, B. Samori, E. Builes, *Biochemistry* **1991**, *30*, 5661 – 5666; b) C. Jordan, L. Lerman, J. Venable, *Nature* **1972**, *236*, 67 – 70; c) F. Livolant, M. F. Maestre, *Biochemistry* **1988**, *27*, 3056 – 3068; d) A. Minsky, *Chirality* **1998**, *10*, 405 – 414; e) Z. Reich, O. Schramm, V. Brumfeld, A. Minsky, *J. Am. Chem. Soc.* **1996**, *118*, 6345 – 6349.
[15] M. F. Maestre, C. Reich, *Biochemistry* **1980**, *19*, 5214 – 5223.

